TECHNOLOGIE 5G

Bulletin de veille scientifique : Novembre 2025

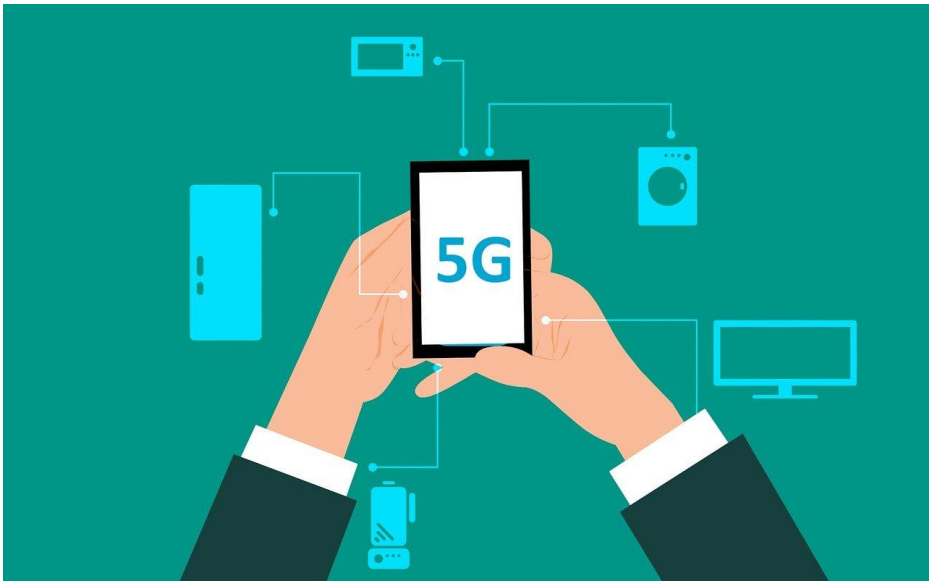

Objectifs : réaliser une veille scientifique sur la technologie 5G

La validation des informations fournies (exactitude, fiabilité, pertinence par rapport aux principes de prévention, etc.) est du ressort des auteurs des articles signalés dans la veille. Les informations ne sont pas le reflet de la position de l'INRS. Les éléments issus de cette veille sont fournis sans garantie d'exhaustivité. Les liens mentionnés dans le bulletin donnent accès aux documents sous réserve d'un abonnement à la ressource.

Les bulletins de veille sont disponibles sur le portail documentaire de l'INRS. L'abonnement permet de recevoir une alerte mail lors de la publication d'un nouveau bulletin (bouton « M'abonner » disponible après connexion à son compte).

Généralités

Quelling Concerns About Rooftops: Do Risk-Communication Strategies Influence Public Acceptance of 5G Base Stations in China?

Liu Y, Qin C. *Risk Anal*. 2025 Nov 7.

The rapid and nationwide expansion of fifth-generation (5G) wireless cellular technology infrastructure in China has prompted serious public concerns, predominantly due to the potential adverse health effects of electromagnetic field (EMF) exposure from 5G base stations. The literature offers mixed results regarding the effectiveness of risk communication on public concerns about EMF exposure from base stations. An online survey experiment with 815 adults in Shanghai examined how different strategies of risk communication could enhance public acceptance. We manipulated the framing of intervention materials (loss- vs. gain-framed) and their information source (government, industry, or civil society). Our analysis revealed that government and industry sources, compared to civil society, were more effective in increasing public support. Additionally, gain frames generated more acceptance than loss frames. Furthermore, participants held higher levels of competence-based trust in government and industry, but no significant difference in care-based trust was detected between government and the other two sources. Both dimensions of trust were critical for public acceptance. These results suggest that the Chinese government, along with professional private sectors, could leverage emerging media platforms to foster support. These results also highlight the need for the Chinese government to address the lack of public care-based trust, especially in the context of centralized 5G deployment.

Lien vers l'article

Performances et sécurité

A Dynamic QoS Mapping Algorithm for 5G-TSN Converged Networks Based on Weighted Fuzzy C-Means and Three-Way Decision Theory.

Wu Y, Xu F, Ning L, Liu X, Chen H, Lu X, et al. *Sensors (Basel)*. 2025 Oct 30;25(21).

To ensure end-to-end Quality of Service (QoS) management in 5G-TSN converged networks, this paper proposes a dynamic weighted QoS mapping method based on Weighted Fuzzy C-Means and Three-Way Decisions (WFCM-TDwQM). The WFCM algorithm is employed to cluster Time-Sensitive Networking (TSN) flows based on their QoS attributes, reducing computational complexity. A three-way decision-based method is used to assign a reasonable and approximate set of 5G QoS Identifier (5QI) values to each cluster. Finally, dynamic weights are adjusted by considering QoS similarity and the residual load rate, enabling the system to adapt to network load changes. The experimental results show that, compared with three other mapping algorithm combinations, WFCM-TDwQM not only ensures end-to-end QoS consistency but also achieves better load balancing under varying network loads. Moreover, its mapping performance is evaluated under different network scenarios.

Lien vers l'article

Hybrid cryptographic approach for strengthening IoT and 5G/B5G network security.

Kumar A, Singh P, Kamble DP, Singh I. *Sci Rep*. 2025 Oct 30;15(1):37971.

The rapid evolution of fifth-generation (5G) and beyond (B5G) networks has introduced significant security challenges, necessitating advanced cryptographic mechanisms to protect sensitive data during transmission. Traditional encryption models often struggle to balance security, computational efficiency, and adaptability to dynamic network conditions. This study proposes a novel hybrid cryptographic framework integrating the Advanced Encryption Standard (AES), Data Encryption Standard (DES), and Rivest-Shamir-Adleman (RSA) algorithms. AES and DES provide high-speed symmetric encryption for efficient data protection, while RSA enables secure key exchange and authentication. The integration of dynamic round keys enhances encryption complexity, improving resistance to cryptanalytic attacks. Performance evaluations, including encryption and decryption time analysis, data expansion metrics, and throughput assessments, demonstrate that the proposed framework achieves an optimal balance between security and computational overhead. Benchmark comparisons with traditional and post-quantum cryptographic models highlight the superior efficiency and reduced data expansion of the hybrid approach. Furthermore, practical implementation on ESP32 hardware confirms the model's feasibility for real-time encryption in resource-constrained environments typical of 5G applications. This scalable and flexible encryption paradigm addresses current and emerging security requirements in high-speed wireless networks, with future work focusing on integration with quantum-resistant cryptographic mechanisms to enhance resilience against evolving cyber threats. Experimental results show that the hybrid model achieves up to 30% higher throughput, 10-15% lower data expansion, and reduced encryption/decryption time compared to baseline algorithms, with successful ESP32 implementation and 100% decryption accuracy for key sizes up to 128 bits.

Lien vers l'article

DL-AoD Estimation-Based 5G Positioning Using Directionally Transmitted Synchronization Signals.

Müürsepp I, Alam MM. *Sensors (Basel)*. 2025 Oct 15;25(20).

This paper introduces a method for estimating the Downlink Angle of Departure (DL-AoD) of 5G User Equipment (UE) from measured signal strengths of directionally transmitted synchronization signals. Based on estimated DL-AoD values, from two or more anchor nodes, the position of the UE was estimated. Unlike most prior work, which is simulation-based or relies on custom testbeds, this study uses real measurements from an operational 5G network in an industrial factory environment. A deterministic estimator was derived, but multipath and unknown beam characteristics limit its accuracy. To address this, machine learning was applied to automatically adapt to the environment. Previous simulation studies reported 90th-percentile DL-AoD estimation errors below 2°, while experimental works achieved best-case accuracies of 5-6°. In this study, the experimental DL-AoD estimation error remained below 4° for 90% of the measurements, indicating improved real-world performance. Reported positioning errors in the literature range from 3.8 m to 140 m, whereas the 13.2 m error obtained here lies near the midpoint of this range, confirming the practicality of the proposed method in industrial environments. Compared to existing approaches, this work demonstrates high angular accuracy using only sub-6 GHz beams in a realistic industrial scenario without detailed knowledge of antenna beam patterns and channel state. The findings demonstrate that standard 5G signals can provide accurate indoor localization without additional infrastructure, offering a practical path toward cost-effective positioning in industrial IoT and automation.

Lien vers l'article

Antennes

A seven-band co-integrated antenna for 5G/6G operations in sub-6 GHz and millimeter-wave frequencies.

Islam MK, Alam MN, Araujo CA, Alwan EA. *Sci Rep*. 2025 Nov 4;15(1):38624.

The use of millimeter-wave (mmWave) frequencies is increasing to meet the broader application needs of modern civilization. These bands are essential in 5G and beyond (Next-G) communication systems to provide wide bandwidth and high data rates. However, it is highly unlikely that the sub-6 GHz bands will be decommissioned anytime soon because of their long-range coverage and high-speed connectivity. Therefore, mmWave and sub-6 GHz antennas and radio frequency (RF) front ends must be integrated into the same system in modern radio designs. Placing various antennas on a single platform is challenging because of the different sizes of the radiating elements that correspond to a wide range of frequencies. To avoid higher-order mode coupling, high isolation is achieved by properly optimizing the placement of each aperture. In this work, we present a co-integrated shared-aperture antenna system capable of operating at seven frequency bands from 600 MHz to 39 GHz, covering both sub-6 GHz and mmWave spectra. Sub-6 GHz operation is achieved using four inverted-L antennas and a slotted patch covering 600 MHz to 6 GHz, while two 4×4 patch arrays are used at 28 GHz and 39 GHz for mmWave. A fabricated prototype demonstrates excellent agreement between measured and simulated results, with consistently low crosstalk (typically below -20 dB), stable realized gain, and compact overall size (200 mm × 85 mm). The proposed design ensures broad frequency coverage and compact integration, making it suitable for 5G/6G, satellite, vehicular, fixed wireless access, IAB, and defense applications requiring multi-band connectivity.

Lien vers l'article

Broadband High-Gain Dual-Polarized Filtering Antenna Using a Partially Reflective Surface Lens for 5G Millimeter-Wave Sensor Applications.

Zhang Y, Liu H. *Sensors (Basel)*. 2025 Nov 4;25(21).

This paper presents a dual-polarized millimeter-wave filtering antenna based on a broadband partially reflective surface lens for gain improvement. It consists of a magneto-electric dipole (M-E dipole) as the source and a partially reflective surface (PRS) as the lens. The M-E dipole source antenna employs a dual-layer substrate structure, and its working principle is investigated by the circuit analysis method. A stub-loaded transmission line network is used to study the radiation characteristics of the source antenna, and the simulation results reveal that it has intrinsic integrated bandpass-type filtering response. The PRS lens is realized by designing a square high permittivity superstrate. By combining the source antenna and the lens, a wideband dual-polarized high gain cavity antenna is developed. The fabricated prototype has a measured impedance bandwidth of 33.3% (25-35 GHz), and a maximum in-band gain of 12.3 dBi. Above features make the proposed antenna a good candidate for 5G millimeter-wave sensor applications.

Lien vers l'article

Design and experimental validation of a compact inverted l-based quad-port MIMO antenna for 5G NR mm wave systems.

Singh AK, Dwivedi AK, Singh V, Pandey A. *Sci Rep*. 2025 Nov 25;15(1):41820.

This paper presents a miniaturized (13x13x0.8 mm(3)) quad-port MIMO antenna for 5G NR n257, n258, & n261 for mm-wave usage. The recommended antenna designed at 29 GHz chose an optimal design (Stage 3) after a careful examination of performance at numerous stages. The single radiating plane consists of an inverted L-shaped design with identical hexagonal slotted loaded DGS. The quad components of the MIMO antenna are set orthogonally for best inter-element mutual coupling. The key feature of the recommended design is (a) impedance bandwidth of 25 -29.5 GHz (Simulated) and 25 to 27.5 GHz or 28 to 29 (measured), along with outstanding mutual coupling of > 25 dB suitable for new radio frequency (RF) bands n257, n258, & n261 (b) an impressive peak gain of 9.5 dB at a full band. Diversity parameters, such as the envelope correlation coefficient (ECC), diversity gain (DG), TARC and channel capacity loss (CCL) are analyzed and calculated the performance characteristics of the proposed MIMO antenna. The suggested antenna's findings have been confirmed by experimental data and have been shown to be in close proximity to the simulated results.

Lien vers l'article

Dual and wideband mmWave 28/38 GHz quad port MIMO antenna for 5G and beyond applications.

Sethumadhavi R, Mishra B, Singh AK, Yadav D, Eduru S, Satheesha TY. *Sci Rep*. 2025 Nov 22.

The current study demonstrates a dual and wideband mmWave 4 × 4 port MIMO antenna for 5G and beyond applications. The proposed antenna is derived from a traditional inset-fed rectangular geometry, modified with multiple curved edges on the top plane to produce a large effective aperture and enable significant surface current distribution. Partial ground planes are connected using 45° tilted conducting strips to form a common ground, which enhances surface current distribution and balances power through each port. The antenna exhibits wide bandwidths of 2.3-6.5 GHz at resonant frequencies of 28-38 GHz, respectively. Moreover, the suggested antenna yields more than 21 dB

isolation, 8.3 dB peak gain, 92% radiation efficiency, 89% multiplexing efficiency, an ECC of 0.00007, and a channel capacity of 21 bit/s/Hz. To validate the antenna design, the prototype was fabricated on a Rogers RT/Duroid 5880™ substrate, tested, and compared with simulated results, showing good agreement.

Lien vers l'article

Correction: High-efficiency dual-band switched beam antenna with back lobe suppression using parasitic elements and patch etching for 5G.

Chaipanya P, Kongka W, Wongpanyanurak N, Wongplueksa C, Thongnuam N, Suksaart W, et al. *Sci Rep*. 2025 Nov 5;15(1):38662.

The original version of this Article contained errors in Figure 3, where panels (a-d) were duplicated from Figure 2. The correct Figure 3 comprises panels (a–c).The original Figure 3 and accompanying legend appear in this article.

Lien vers l'article

Architecture réseau

Design and Performance Analysis of Sub-THz/THz Mini-Cluster Architectures for Dense Urban 5G/6G Networks.

Farré V, Vega-Sánchez J, Garzón V, Garzón NO, Mora HC, Benitez Olivo EE. *Sensors (Basel)*. 2025 Nov 3;25(21).

The transition from Fifth Generation (5G) New Radio (NR) systems to Beyond 5G (B5G) and Sixth Generation (6G) networks requires innovative architectures capable of supporting ultra-high data rates, sub-millisecond latency, and massive connection densities in dense urban environments. This paper proposes a comprehensive design methodology for a mini-cluster architecture operating in sub-THz (0.1-0.3 THz) and THz (0.3-3 THz) frequency bands. The proposed framework aims to enhance existing 5G infrastructure while enabling B5G/6G capabilities, with a particular focus on hotspot coverage and mission-critical applications in dense urban environments. The architecture integrates mini Base Stations (mBS), Distributed Edge Computing Units (DECUs), and Intelligent Reflecting Surfaces (IRS) for coverage enhancement and blockage mitigation. Detailed link budget analysis, coverage and capacity planning, and propagation modeling tailored to complex urban morphologies are performed for representative case study cities, Quito and Guayaquil (Ecuador). Simulation results demonstrate up to 100 Gbps peak data rates, sub 100 µs latency, and tenfold energy efficiency gains over conventional 5G deployments. Additionally, the proposed framework highlights the growing importance of THz communications in the 5G evolution towards B5G and 6G systems, where ultra-dense, low-latency, and energy-efficient mini-cluster deployments play a key role in enabling next-generation connectivity for critical and immersive services. Beyond the studied cities, the proposed framework can be generalized to other metropolitan areas facing similar propagation and capacity challenges, providing a scalable pathway for early-stage sub-THz/THz deployments in B5G/6G networks.

Lien vers l'article

Efficacité énergétique

Aucun article dans ce bulletin.

Autres équipements

Design and Preparation of Compact 3-Bit Reconfigurable RF MEMS Attenuators for Millimeter-Wave Bands.

Miao S, Chai R, Si Y, Zhang Y, Wu Q, Li M. *Micromachines (Basel)*. 2025 Sep 29;16(10).

As a core functional device in microwave systems, attenuators play a crucial role in key aspects such as signal power regulation, amplitude attenuation, and impedance matching. Addressing the pressing technical issues currently exposed by attenuators in practical applications, such as excessive insertion loss, low attenuation accuracy, large physical dimensions, and insufficient process reliability, this paper proposes a design scheme for an RF three-bit reconfigurable stepped attenuator based on radio frequency micro-electromechanical systems (RF MEMS) switches. The attenuator employs planar integration of the T-type attenuation network, Coplanar Waveguide (CPW), Y-shaped power divider, and RF MEMS switches. While ensuring rational power distribution and stable attenuation performance over the full bandwidth, it reduces the number of switches to suppress parasitic parameters, thereby enhancing process feasibility. Test results confirm that this device demonstrates significant advancements in attenuation accuracy, achieving a precision of 1.18 dB across the 0-25 dB operational range from DC to 20 GHz, with insertion loss kept below 1.65 dB and return loss exceeding 12.15 dB. Additionally, the device boasts a compact size of merely 0.66 mm × 1.38 mm × 0.32 mm, significantly smaller than analogous products documented in existing literature. Meanwhile, its service life approaches 5 × 10(7) cycles. Together, these two attributes validate the device's performance reliability and miniaturization advantages.

Lien vers l'article

Small scale lowpass and quad-band bandpass filter for 5G application.

Choudhary DK, Pratap K. *Sci Rep*. 2025 Nov 25;15(1):41922.

This work offers a new small-scaled lowpass and quad-band passband filter with low insertion loss and high selectivity. By integrating a shorted interdigital capacitor (IDC), closed ring resonator, meander line, and rectangular-shaped virtual ground plane, better impedance matching and transmission properties have been attained. Initially, the lowpass response structure comprises shorted IDC and closed ring resonators. Further utilizing pairs of meander lines and rectangular stubs on both sides of ring resonators, a quad bandpass along with a lowpass filter was constructed. Excluding the fifty-ohm feedline the proposed filter area measures only 0.04λ(g) × 0.06λ(g) (15.6 mm×24.6 mm) at the lowpass frequency of 3dB cutoff, 0.75 GHz. The fractional bandwidth at 3-dB of the proposed four passband zones are 63.76% (1.39-2.78 GHz), 22.55% (3.26-4.09 GHz), 17.15% (4.42-5.24 GHz), and 4.3% (5.64-5.89 GHz) at operating frequencies of 02.18, 3.68, 4.78 and 5.82 GHz, respectively. Moreover, the resonance frequencies of each band can be adjusted by altering the structural parameters of the intended filter, which results in modifications to their relative lumped parameters. By doing

experimental measurements that correlate with simulated ones, the suggested filter is validated. The designed filter may be useful for 5G communication frequency range-1 (FR1), 0.45-6.0 GHz bands.

Lien vers l'article

Applications médicales et industrielles de la 5G

Applications industrielles

Aucun article dans ce bulletin.

Applications médicales

Toward safe clinical deployment of remote robotic surgery in Japan: five-year validation of the hinotori™ system using 5G wireless communication.

Hara T, Morihiro Y, Horise Y, Komatsu S, Ohashi M, Kitatsuji H, et al. *Int J Clin Oncol*. 2025 Dec;30(12):2389-98.

Remote robotic-assisted surgery (RRAS), a form of telesurgery, offers a potential solution to Japan's surgeon shortage and regional disparities in care. Despite advances in robotic systems and modern communication technologies, including both 5G wireless and wired networks, clinical adoption remains limited due to regulatory, infrastructural, and institutional barriers. This review consolidates five years (2020-2025) of technical and operational validation of the hinotori™ Surgical Robot System-a domestically developed platform-in alignment with the 2022 Japanese Remote Surgery Guidelines. Based on over 30 remote-session evaluations by Kobe University, Medicaroid, and NTT DOCOMO, we summarize system performance across key domains: communication latency, QoS-based prioritization, VPN redundancy, fail-safe mechanisms, electromagnetic compatibility, human-system interaction, and legal compliance. Under optimized Sub6 5G SA conditions, the system consistently achieved a round-trip latency of approximately 100 ms and stable stereoscopic video transmission, even during simulated 1 Gbps congestion. Safety was ensured through automatic standby, dual-cockpit fallback, and real-time monitoring. Although hinotori™ meets technical and safety criteria, full-scale implementation remains constrained by legal requirements-particularly the mandate for an on-site physician under Article 20 of the Medical Practitioners Act. Supervised telesurgery, where remote surgeons assist on-site teams, is legally permissible and may serve as a transitional model. This review integrates technical findings with policy considerations, proposing a path toward safe, equitable, and sustainable RRAS deployment in Japan. To our knowledge, this is the first comprehensive review aligning domestic telesurgical validation with national policy benchmarks, offering a foundation for future regulation, accreditation, and digital surgical integration.

Lien vers l'article

Application of 5G-powered robot-assisted teleultrasound diagnostic system in percutaneous nephrolithotomy under the one-to-many mode: ensuring safety, enhancing efficacy, and advancing surgical training.

Lu R, Zhou X, Xu Z, Chen S, Wu W, Jiang K, et al. *World J Urol*. 2025 Nov 13;43(1):689.

OBJECTIVE: This study investigates the safety, efficacy, and educational potential of the 5G-powered robot-assisted teleultrasound diagnostic system (RTDS) for guiding percutaneous nephrolithotomy (PCNL) in a one-to-many telemedicine model, addressing medical resource disparities in remote

regions. METHODS: Forty-five patients with complex kidney stones (Guy's Stone Scores III-IV) underwent RTDS-assisted PCNL across multiple regions (Xinjiang, Chongqing, Liyang, Suqian), with a maximum distance of 5800 km. Experts from the First Affiliated Hospital of Nanjing Medical University remotely operated the RTDS to assist local surgeons in establishing percutaneous renal access. Primary endpoints included one-session stone-free rate (SFR), first puncture success rate, and Clavien-Dindo complication rate. Secondary endpoints, such as operative time and hemoglobin drop, were also evaluated. Subjective assessments of surgeon workload and emotional state were conducted using the NASA Task Load Index (NASA TLX) and Medical Emotion Scale (MES). For contextual comparison, a systematic review and meta-analysis of published studies on conventional ultrasound-guided PCNL was conducted. RESULTS: The one-session stone-free rate (SFR) reached 80%, with a first-puncture success rate of 76.9%. No complications above grade II were observed, and the complication rate (8.9%) was lower than traditional ultrasound-guided PCNL (16%). Meta-analysis revealed RTDS had comparable SFR but superior safety and first puncture success rates. Surgeons reported reduced intraoperative workload and heightened confidence, underscoring RTDS's educational utility. The one-to-many telemedicine mode exhibited stable performance, facilitating simultaneous real-time guidance for multiple surgeries in geographically dispersed locations. CONCLUSIONS: The 5G-powered RTDS is a safe, effective, and innovative tool for guiding PCNL. It not only bridges healthcare disparities by providing high-quality medical services in remote regions but also enhances the training of junior surgeons, promoting the equitable development of advanced surgical techniques. This study primarily reports original prospective clinical data. The supplementary meta-analysis serves only as contextual reference and should not be interpreted as a substitute for randomized controlled trials.

Lien vers l'article

Evaluation (Mesure des niveaux d'exposition)

Méthodes d'évaluation

Aucun article dans ce bulletin.

Evaluation population générale

Comprehensive Measurement-Based Assessment of Downlink RF-EMF Exposure in Urban Environments: Multi-Method Analysis and Intercomparison.

Wang S, Zhang Y, Liu Y, Liu J, Conil E, Jawad O, et al. *Bioelectromagnetics*. 2025 Dec;46(8):e70033.

This paper presents a comprehensive measurement-based assessment of radio-frequency (RF) electromagnetic field (EMF) exposure level in a French city. Three types of assessment methods are used to collect measurement data: drive test (DT), spot measurements, and sensor networks. The DT measurements were conducted by a portable spectrum analyzer, i.e., Tektronix RSA 306B, connected to a 3-axis antenna mounted on the roof of the vehicle. DT system continuously recorded frequency-dependent electric field (E-field) values on a pre-defined outdoor route. The spot measurements were done in the same region, covered by DT, with both broadband and frequency-selective systems. Additionally, 19 sensors were installed on streetlamps in the same part of the city to measure the broadband E-field level. The overall statistical analysis on raw data shows good agreement on RF-EMF exposure level from three types of measurements. Then a distance-based moving average method was carried out to remove the random noise in the DT data, where the optimized window size is explored using Kolmogorov-Smirnov test. The smoothed DT data show a good correlation with nearby spot measurement values, as well as with base station antenna (BSA) density. Specific fifth-generation (5G) spot measurements, performed with and without traffic-attracting downloads, demonstrate the impact of beamforming on exposure levels in 5G new radio (NR) bands. Then spot measurements were used to build the exposure map using the kriging method, where the kriging prediction from the trained model is further compared with DT. Furthermore, the temporal variations observed in the sensor network were analyzed in relation to distance from the nearest BSA, revealing an inverse proportional relationship between E-field level and proximity to the nearest BSA. This study shows good reliability in assessing the RF-EMF exposure level using different systems. The advantages and limitations of different systems are also demonstrated by performing the intercomparison between data sets.

Lien vers l'article

Exposure Variability Between 1- or 6-Minute and 30-Minute Averaging Time Lengths in Radiofrequency-Electromagnetic Field Exposure Monitoring.

Bhatt CR, Henderson S, Sanagou M, Loughran S. *Bioelectromagnetics*. 2025 Dec;46(8):e70030.

Different averaging time lengths (ATLs) are widely used in radiofrequency-electromagnetic field (RF-EMF) exposure monitoring. This study evaluated variability in RF-EMF exposure associated with the ATLs of 1- and 6-min normalised to 30-min data. For 15 frequency bands of interest, RF-EMF exposures

were collected in contiguous 1-min blocks over 30 min at four sites (two outdoor and two indoor). Frequency-band and site-specific variability in exposure between the three ATLs was assessed. First, the variability in terms of relative deviation (in dB) between 1- or 6-min and 30-min were estimated. Second, the overall exposure variability (in µW/m(2)) were compared between 1- or 6-min and 30-min blocks statistically using the quantile regression method. The overall exposure variability on ATL of 1-min or 6-min was considered different to 30-min if a majority of respective sub-pair comparisons across different percentiles (P(5), P(25), P(50), P(75), P(95)) were significantly different. The study largely showed that the exposure variability (i.e., relative deviation) of different ATLs was within +/- 3 dB. Further, the overall exposure variability between 1- or 6-min and 30-min ATLs showed inconsistent outcomes. Frequency bands of broadcast and most of the mobile services < 2 GHz demonstrated overall similar exposure variability for 1-min and 6-min ATLs.

Lien vers l'article

Risques professionnels

Aucun article dans ce bulletin.

Effets biologiques et sur la santé

In silico

Aucun article dans ce bulletin.

In vitro

Radiofrequency regulates the BET-mediated pathways in radial glia differentiation in human cortical development.

Cakir B, Tanaka Y, Choe MS, Kiral FR, Kim J, Micali N, et al. *Cell Rep*. 2025 Oct 28;44(10):116238.

The human brain represents one of the most complex organs in our body, with development regulated by an intricate genetic program. Recently, non-genetic factors, such as prenatal stress, infection, and diet, have been shown to influence brain development. Radiofrequency radiation (RF; 800-2,400 MHz), emitted by natural and artificial sources such as microwaves and cell phones, represents a non-invasive environmental factor. Using human cortical organoids (hCOs) derived from human embryonic stem cells (hESCs), we investigate RF's effects on corticogenesis. We find that RF exposure regulates the differentiation of human and non-human primate radial glia progenitors, maintaining stem cell identity and delaying differentiation. Neurons differentiated under RF treatment show induction of expression of human endogenous retroviruses. Importantly, inhibitors for the BET (bromodomain and extraterminal) protein rescue RF-induced developmental defects in hCOs. Our findings reveal a mechanism by which RF modulates early brain development, offering a non-biological approach to regulate neural stem cell self-renewal.

Lien vers l'article

Sur l'animal

Prolonged 3.5 GHz and 24 GHz RF-EMF Exposure Alters Testicular Immune Balance, Apoptotic Gene Expression, and Sperm Function in Rats.

Syed Taha SMA, Jaffar FHF, Hairulazam A, Vijay S, Jamaludin N, Zulkifli AF, et al. *Biomedicines*. 2025 Oct 11;13(10).

Background/Objectives: The rapid rollout of 5G has renewed interest in potential reproductive effects of mid-band (3.5 GHz) and millimeter-wave (24 GHz) radiofrequency electromagnetic fields (RF-EMF). We examined frequency- and duration-dependent changes in testicular cytokines, apoptosis-related genes, and sperm quality in rats. Methods: Male Sprague Dawley rats (n = 6 per group) were exposed for 60 days to 3.5 GHz or 24 GHz RF-EMF for 1 h/day or 7 h/day. The sham controls were housed identically. Testicular expressions of IL-10, IL-6, IL-1β, and TNF-α were quantified; Tp53, Bax, Bcl2, and Casp3 mRNA expressions were measured; and sperm concentration, viability, and motility were evaluated. Results: IL-10 was significantly reduced in the 24 GHz group at both 1-h and 7-h exposure duration. At 7 h, TNF-α was also lower at 24 GHz. Casp3 expression was higher and Tp53 was lower at

3.5 GHz at 1-h exposure duration. Sperm concentration and viability were reduced after 24 GHz exposure at 7 h, while sperm motility was reduced after 3.5 GHz exposure at both durations. Conclusions: Exposure to RF-EMF 3.5 GHz primarily impacts sperm motility via extrinsic pro-apoptotic pathways, while exposure to 24 GHz impacts sperm concentration and viability potentially through immune-apoptotic mechanisms, with all negative effects amplified by 7-h daily exposure.

Lien vers l'article

Sur l'homme

Millimeter-wave high frequency 5G (26 GHz) electromagnetic fields do not modulate human brain electrical activity.

Michelant L, Baz T, Carrie A, Hugueville L, Lévêque P, Selmaoui B. *Environ Res*. 2025 Nov 18:123349.

The deployment of 5G networks utilizing millimeter-wave frequencies such as 26 GHz has raised concerns about potential neurophysiological effects. However, no controlled studies have investigated the impact of 26 GHz exposure on human brain electrical activity. We conducted a randomized, triple-blind crossover study in 31 healthy young adults (18 men, 14 women, mean age 26.1 ± 5.2 years). Participants underwent two sessions (real and sham exposure) separated by one week, with 26.5-minute exposure to 26 GHz electromagnetic fields at 2 V/m. EEG activity was recorded before, during, and after exposure. Power spectral density was computed for delta (1-4 Hz), theta (4-8 Hz), alpha (8-12 Hz), and beta (12-35 Hz) frequency bands. Statistical analysis employed mixed-effects models with baseline correction, examining exposure effects across temporal phases and electrode clusters. No significant modulation of EEG frequency bands was observed during eyes-closed conditions following 26 GHz exposure. Mixed-effects modeling revealed no significant main effects or interactions for exposure conditions across all frequency bands and electrode clusters. This first controlled investigation of 26 GHz 5G effects on human EEG activity found no detectable alterations in brain electrical activity under regulatory-compliant exposure conditions. These findings contribute important preliminary safety data for 5G millimeter-wave technology deployment, though further research across diverse populations and exposure scenarios remains warranted.

Lien vers l'article

Reproduction

Non-thermal biological effects of radiofrequency electromagnetic radiation: Mechanistic insights into male reproductive vulnerability in the era of ubiquitous exposure.

Jangid P, Rai U, Ahmed S, Singh S, Singh R. *Reprod Toxicol*. 2025 Dec;138:109087.

The rapid proliferation of wireless technologies has led to continuous, low-intensity exposure to radiofrequency electromagnetic radiation (RF-EMR) from devices such as mobile phones, Wi-Fi routers, and wearable electronics. Although RF-EMR is non-ionizing, a growing body of evidence indicates that chronic exposure can induce non-thermal biological effects with significant implications for male reproductive health. This review synthesizes current findings on the mechanistic pathways through which RF-EMR may impair fertility, focusing on oxidative stress, mitochondrial dysfunction, DNA damage, apoptosis, autophagy dysregulation, and hormonal disruption via hypothalamic-pituitary-gonadal (HPG) axis interference. Experimental and clinical studies consistently link RF-EMR exposure to reduced sperm count and motility, altered testicular architecture, blood-testis barrier compromise, and suppressed testosterone synthesis, often at specific absorption rates below current safety thresholds. These outcomes are underpinned by redox imbalance, mitochondrial collapse, and steroidogenic impairment, with emerging evidence for epigenetic and transgenerational effects. Existing regulatory frameworks, based largely on thermal safety limits, fail to address the complexity of real-world, multi-source, long-term exposures. The review highlights critical knowledge gaps, particularly regarding 5 G and millimeter-wave frequencies, and underscores the need for standardized research protocols, biologically relevant exposure metrics, and precautionary public health measures to mitigate reproductive risks in an increasingly wireless environment.

Lien vers l'article

Investigation of fetal exposure to electromagnetic waves between 2.45 and 5 GHz during pregnancy.

İl N, Ateş K, Özen Ş. *Radiat Prot Dosimetry*. 2025 Nov 1;201(18):1188-200.

In this paper, we have assessed the specific absorption rate (SAR) in fetal brain and lungs during the second trimester of pregnancy conditions of body exposure to radiofrequency electromagnetic field (RF-EMF). SAR calculations were performed for frontal and lateral incidences, with both vertical and horizontal polarization of the incident electromagnetic (EM) waves at frequencies ranging from 2.45 to 5 GHz. A realistic pregnant human model with a belly button piercing was implemented for numerical simulation for nonionizing dosimetry. The simulation results reveal that SAR tends to rise in the presence of belly-button piercing. The highest SAR10g recorded on the fetus's lungs was 16 mW/kg at a frequency of 2.45 GHz. Similarly, the maximum SAR10g value on the fetus's brain was measured 14 mW/kg, occurring at a frequency of 2.45 GHz. Results indicate that metal objects can lead to an increase in SAR values. However, obtained values remain below limits set by international organizations like the Institute of Electrical and Electronics Engineers and the International Commission on Non-Ionizing Radiation Protection.

Lien vers l'article

Dispositifs médicaux implantables

Aucun article dans ce bulletin.